

# Characterization and catalytic activity of 2,6-dichlorophenyl substituted iron(III) porphyrin supported on silica gel and imidazole propyl gel

Yassuko Iamamoto<sup>a,\*</sup>, Kátia J. Ciuffi<sup>a,c</sup>, Hérica C. Sacco<sup>a,c</sup>, Lídia S. Iwamoto<sup>a,c</sup>,  
Otaciro R. Nascimento<sup>b</sup>, Cynthia M.C. Prado<sup>a</sup>

<sup>a</sup> Departamento de Química, FFCLRP, Universidade de São Paulo, Av. Bandeirantes, 3900, CEP 14040-901, Ribeirão Preto, SP, Brazil

<sup>b</sup> Instituto de Física de São Carlos, Universidade de São Paulo, São Carlos, SP, Brazil

<sup>c</sup> Instituto de Química, UNESP, Araraquara, SP, Brazil

Received 30 May 1996; accepted 22 July 1996

## Abstract

In this work we have made use of the study of the interaction between Fe(TDCPP)<sup>+</sup> and the axial ligands OH<sup>-</sup> and imidazole in order to help characterize the heterogenized catalysts Fe(TDCPP)SG and Fe(TDCPP)IPG through UV–VIS and EPR spectroscopies and thus, better understand their different catalytic activity in the oxidation of cyclohexane by PhIO. We have found out that in Fe(TDCPP)SG (containing  $1.2 \times 10^{-6}$  mol Fe(TDCPP)<sup>+</sup>/g of support), the FeP bis-coordinates to silica gel through Fe–O coordination and it is high-spin Fe<sup>III</sup>P species. In Fe(TDCPP)IPG **1** (containing  $1.1 \times 10^{-6}$  mol Fe(TDCPP)<sup>+</sup> and  $2.2 \times 10^{-4}$  mol imidazole/g of support), the FeP is bis-ligated to imidazole propyl gel through Fe-imidazole coordination and using NO as a paramagnetic probe, we present evidence that Fe(TDCPP)<sup>+</sup> is present as a mixture of low-spin Fe<sup>III</sup>P and Fe<sup>II</sup>P species. This catalyst led to a relative low yield of cyclohexanol (25%) because the bis-coordination of the Fe<sup>III</sup>P to the support partially blocks the reaction between Fe(TDCPP)<sup>+</sup> and PhIO, thus leading to the formation of only a small amount of the active species Fe<sup>IV</sup>(O)P<sup>++</sup>, while the Fe<sup>II</sup>P species do not react with the oxygen donor. Increasing the amount of Fe(TDCPP)<sup>+</sup> and decreasing the amount of imidazole in the support led to the obtention of high-spin Fe<sup>III</sup>P EPR signals in the spectra of Fe(TDCPP)IPG **5** (containing  $4.4 \times 10^{-6}$  mol Fe(TDCPP)<sup>+</sup> and  $2.2 \times 10^{-5}$  mol imidazole/g of IPG), together with low-spin Fe<sup>III</sup>P species. This latter catalyst led to better cyclohexanol yields (67%) than Fe(TDCPP)IPG **1**. Fe(TDCPP)IPG **5** was further used in a study of the optimization of its catalytic activity and in recycling experiments in the optimized conditions. Recycling oxidation reactions of Fe(TDCPP)IPG **5** led to a total turnover number of 201 and total cyclohexanol yield of 201%, which could not be attained with Fe(TDCPP)Cl in homogeneous solution (turnover = 96) due to the difficulty in recovering and reusing it.

**Keywords:** Cyclohexane; Imidazole propyl gel; Iron(III)porphyrin; 2,6-dichlorophenyl porphyrin; Oxidation; Porphyrin; Supported catalysts

## 1. Introduction

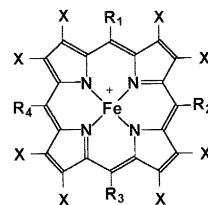
The cytochrome P-450 dependent mono-oxygenases have attracted much interest in recent years, since they are able to catalyze the

\* Corresponding author. Tel.: +55-16-6331010; fax: +55-16-6338151; e-mail: iamamoto@usp.br.

selective monooxygenation of a wide variety of organic substrates under mild conditions, using  $O_2$  and NADPH in living organisms or single oxygen atom donors such as iodosylarenes in vitro [1–4]. Great advances have been made towards the understanding of these processes through studies on the biological systems and also on inherently simpler chemical models. This in turn has led chemists to consider whether these enzymes might provide the key to the development of new catalysts for organic oxidations [5]. In fact, the finding of catalysts capable of oxidizing saturated hydrocarbons selectively and efficiently under mild conditions is particularly desirable because, despite the fact that alkanes and cycloalkanes are among the main products of the petrochemical industry and are present in large quantities in nature, they are rarely used as raw material in fine and industrial chemistry due to the inertness of the C–H bonds [6,7].

A strategy to developing catalytic systems capable of mimicking the catalytic cycle of the cytochrome P-450 has been the use of metalloporphyrins, which are analog to the prosthetic group of these monooxygenases: iron protoporphyrin IX [6]. The first system described by Groves et al. [8] was based on Fe(TPP)Cl (Fig. 1) and iodosylbenzene (PhIO) in the oxidation of cyclohexane and it was able to mimick all the reactions of the short catalytic cycle of P-450, from a qualitative point of view. More stable and efficient catalysts were further obtained with the introduction of electron-withdrawing substituents in the meso-aryl positions and/or  $\beta$ -pyrrole positions of the tetraphenylporphyrin [6,9–11]. Examples of such catalysts are present in Fig. 1.

However, the cost of these catalysts is such that methods to ensure maximum product output per gram of catalyst have to be developed. If these metalloporphyrin-catalyzed oxidations are to be applied to synthetic procedures for laboratory, medium and large-scale reactions, two important difficulties must be overcome: catalyst recovery and reuse [5]. Therefore, another ap-



Ironporphyrin	$R_1 = R_2 = R_3 = R_4 =$	X =
Fe(TPP) <sup>+</sup>	Ph	H
Fe(TDCPP) <sup>+</sup>	2,6 diClPh	H
Fe(TFPP) <sup>+</sup>	C <sub>6</sub> F <sub>5</sub>	H
Fe(TDCPCl <sub>2</sub> P) <sup>+</sup>	2,6 diCl Ph	Cl

Fig. 1. Iron(III)porphyrins.

proach to enhancing the catalytic activity of metalloporphyrins has been its immobilization on organic (polymers) [12–16] or inorganic (ion exchange resins [17], clays [18,19], zeolites and silica [13–15,20]) matrices, which creates site-isolation. This is suggested as a biomimetic system, since in the natural monooxygenases, the iron protoporphyrin IX is surrounded by the protein matrix, creating site-isolation of the active center [12]. Supporting metalloporphyrins on matrices presents the following advantages: (i) prevention of catalyst intermolecular self-oxidation; (ii) prevention of dimerization of unhindered metalloporphyrins such as Fe(TPP)<sup>+</sup> and Fe(TFPP)<sup>+</sup> and (iii) easy recovery and reuse of the catalyst [16]. Furthermore, in the era of ‘clean technology’, heterogenized catalysts have become an important and attractive target since they represent the possibility of replacing the traditional stoichiometric processes in industry and therefore help to minimize the problems of industrial waste treatment and disposal. Nevertheless, there is one serious problem with these systems: it is difficult to characterize both the catalyst on the surface of the support and the intermediates formed in the catalytic processes by standard techniques. In this way, it is generally assumed that the behavior of the bound catalyst in the oxidation is the same or similar to that of the homogeneous analog, which can be more readily defined [5].

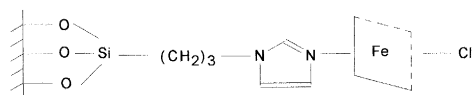


Fig. 2. Ironporphyrin-IPG.

For general application, the supported metalloporphyrin should be oxidatively stable, tough and resistant to physical abrasion, reusable, resistant to metalloporphyrin leaching or removal and suitable for batch or continuous flow systems [5]. Silica (SG) has been an attractive support for metalloporphyrins, since they are inert and oxidatively stable even under drastic conditions [2]. The more common approach to using silica as a coordinative support requires converting the surface silanol groups into silylpropyl derivatives (Fig. 2), which act as ligands for the metalloporphyrin [21–23].

Despite these potential advantages, there have been relatively few studies on oxidations catalyzed by non-ionic metalloporphyrins anchored to silica or modified silicas and on the reuse of such catalysts. Few also have been the reports on the characterization of supported metalloporphyrins.

In 1992 and 1994, Lindsay-Smith et al. [13,23] reported the epoxidation of cyclooctene using  $\text{Fe}(\text{TDCPP})^+$  or  $\text{Fe}(\text{TFPP})^+$  bound to either (1-imidazolyl)methylated polystyrene (PS-Im), poly-4-vinylpyridine (PVP), silica modified with imidazole (IPG) or silica modified with pyridine (Py-Si) and  $\text{Mn}(\text{TDCPP})^+$  bound to PS-Im. In 1994, our research group [24] reported a study on the catalytic activity of  $\text{Fe}(\text{TPP})^+$ ,  $\text{Mn}(\text{TPP})^+$ ,  $\text{Fe}(\text{TDCPP})^+$ ,  $\text{Mn}(\text{TDCPP})^+$  and  $\text{Fe}(\text{TFPP})^+$  supported on either SG or IPG, in the hydroxylation of cyclohexane by PhIO. The reuse of the catalysts  $\text{Fe}(\text{TDCPP})\text{IPG}$ ,  $\text{Fe}(\text{TFPP})\text{IPG}$  and  $\text{Mn}(\text{TDCPP})\text{IPG}$  in these reactions was also reported [24]. In addition, we also reported some results about the characterization of  $\text{Fe}(\text{TDCPP})\text{IPG}$  by UV–VIS and EPR spectroscopy. We found that when  $\text{Fe}(\text{TDCPP})\text{IPG}$  contains  $1.2 \times 10^{-6}$  mol  $\text{Fe}(\text{TDCPP})^+$  and  $2.2$

$\times 10^{-4}$  mol imidazole per gram of IPG ( $\text{Im}/\text{Fe}(\text{TDCPP})^+$  ratio = 200), the iron porphyrin is a mixture of bis-ligated low-spin  $\text{Fe}^{\text{III}}$  and  $\text{Fe}^{\text{II}}$  species. When the amount of porphyrin in the support was increased to  $4.5 \times 10^{-6}$  mol  $\text{Fe}(\text{TDCPP})^+$  per gram of IPG ( $\text{Im}/\text{Fe}(\text{TDCPP})^+$  ratio = 45), the EPR signals for low-spin  $\text{Fe}^{\text{III}}$  decreased and the  $g = 5.985$  signal for high-spin  $\text{Fe}^{\text{III}}$  was detected. When a third  $\text{Fe}(\text{TDCPP})\text{IPG}$  containing  $3.3 \times 10^{-6}$  mol  $\text{Fe}(\text{TDCPP})^+$  and  $2.2 \times 10^{-5}$  mol imidazole per gram of IPG ( $\text{Im}/\text{Fe}(\text{TDCPP})^+$  ratio = 6.7) was used, an EPR spectrum with a more intense  $\text{Fe}^{\text{III}}$  high-spin signal than the previous one was obtained. Comparing the catalytic activity of the three catalysts, the best cyclohexanol yields were obtained with the latter  $\text{Fe}(\text{TDCPP})\text{IPG}$  containing a higher amount of high-spin  $\text{Fe}^{\text{III}}$  and a lower  $\text{Im}/\text{Fe}(\text{TDCPP})^+$  ratio. Therefore, we concluded that excess imidazole in the former  $\text{Fe}(\text{TDCPP})\text{IPG}$  had led to bis-ligation of the  $\text{FeP}$  to the support and to the reduction of the  $\text{Fe}^{\text{III}}$  ion to  $\text{Fe}^{\text{II}}$ , making the catalyst less efficient.

More recently, in 1995, Lindsay-Smith et al. also reported a study about the reuse of the catalyst  $\text{Fe}(\text{TDCPP})\text{Py-Si}$  in the epoxidation of cyclooctene [14] and the characterization of  $\text{Fe}(\text{TFPP})^+$  and  $\text{Fe}(\text{TDCPP})^+$  supported on either PS-Im, PVP, IPG or Si-Py by UV–VIS, Raman resonance and EPR spectroscopies [25]. Lindsay presented evidence that the  $\text{FeP}$  on the flexible organic polymers are all low-spin bis-ligated  $\text{Fe}^{\text{II}}$  species and that  $\text{Fe}(\text{TDCPP})^+$  on Si-Py is low-spin  $\text{Fe}^{\text{II}}$  species as well [25]. With  $\text{Fe}(\text{TDCPP})\text{IPG}$  containing  $4.1 \times 10^{-6}$  mol  $\text{Fe}(\text{TDCPP})^+$  and  $1.3 \times 10^{-3}$  mol imidazole per gram of IPG, Lindsay reports that it presents the  $\text{FeP}$  mono-ligated to the support as high-spin  $\text{Fe}^{\text{III}}$  species [25].  $\text{Fe}(\text{TFPP})^+$  on IPG was found to be a mixture of both oxidation states [25].

In this work, we will continue our study on the characterization of  $\text{Fe}(\text{TDCPP})\text{IPG}$  catalysts containing different amounts of  $\text{Fe}(\text{TDCPP})^+$  and imidazole per gram IPG (thus different  $\text{Im}/\text{Fe}(\text{TDCPP})^+$  ratios) by EPR spectroscopy.

To complement such study, we will also report the characterization of these catalysts by EPR spectroscopy using NO as a paramagnetic probe. Moreover, we will present a study on the optimization of reaction conditions for Fe(TDCPP)IPG as catalyst for cyclohexane hydroxylation, as well as a new study of the reuse of this catalyst in the optimized conditions.

As the nature of the bonding of Fe(TDCPP)<sup>+</sup> to SG is still not clear [5], we have also carried out the characterization of Fe(TDCPP)SG by UV–VIS and EPR spectroscopies.

## 2. Experimental

### 2.1. Materials

Dichloromethane (DCM) and dichloroethane (DCE) were distilled and stored on 4A molecular sieves. Acetonitrile (ACN) and methanol (MeOH) were stored on 3A molecular sieves. *N,N*-dimethylformamide (DMF) was stirred over KOH at room temperature overnight, decanted and then distilled at reduced pressure. The cyclohexane purity was determined by gas chromatographic analysis. Trifluoroethanol (CF<sub>3</sub>CH<sub>2</sub>OH) was used as purchased from Aldrich.

#### 2.1.1. Iodosylbenzene (*PhIO*)

Iodosylbenzene was obtained through the hydrolysis of iodosylbenzenediacetate [26]. Samples were stored in a freezer and the purity was checked every six months by iodometric assay.

#### 2.1.2. Iron(III) meso tetrakis(2,6-dichlorophenylporphyrin) chloride (*Fe(TDCPP)Cl*)

TDCPPH<sub>2</sub> was purchased from Midcentury and iron insertion into the free base was carried out adapting the method described by Adler et al. [27]. DMF was removed by rotary evaporator and the attained Fe(TDCPP)Br ( $\lambda_{\max}$  = (DMF) 392, 418, 508, 570, 642 nm) was washed with water. The attained Fe(TDCPP)<sup>+</sup> ( $\lambda_{\max}$  =

(DCM) 334, 414, 576 nm) was purified by silica column chromatography, using a mixture gradient of 5–10% MeOH in DCM as eluent. The UV–VIS spectrum of Fe(TDCPP)<sup>+</sup> obtained after its purification presented a new absorption band at  $\lambda$  = 578 nm, which replaced the bands at  $\lambda$  = 508, 584 and 644 nm, present in the initial spectrum of Fe(TDCPP)Br. As the band at  $\lambda$  = 578 nm is attributed to FeP–oxygen coordination [28,29], we think that Fe(TDCPP)<sup>+</sup> coordinated to the solvent MeOH used in its purification, leading to its bis-methanol complex. The DCM solution of purified Fe(TDCPP)<sup>+</sup> was bubbled through with hydrogen chloride gas, which converted it to Fe(TDCPP)Cl ( $\lambda_{\max}$  (DCM) = 342, 416, 506, 578, 644 nm).

#### 2.1.3. Solid supports

Silica gel (SG) was dried by heating at 60°C (5 mm Hg) for 4 h. IPG was prepared by the method described by Basolo et al. [21]. IPG containing two different amounts of imidazole per gram of support were prepared: (i) elemental analysis: C = 5.27%, H = 1.20%, N = 0.65%, which corresponds to  $2.2 \times 10^{-4}$  mol imidazole per gram of IPG; (ii) elemental analysis: C = 5.27%, H = 1.05% and N = 0.07%, which corresponds to  $2.2 \times 10^{-5}$  mol imidazole per gram of IPG.

#### 2.1.4. Preparation of supported metalloporphyrins

The Fe(TDCPP)<sup>+</sup> ligation to IPG or SG was achieved by stirring a dichloromethane solution of a known amount of Fe(TDCPP)<sup>+</sup> with a suspension of the support for 10–20 min and the resulting supported catalyst was washed with CH<sub>2</sub>Cl<sub>2</sub> (3 portions of 2 mL) to remove unbound and weakly bound porphyrin. The solid catalyst was then dried for 3 h at 60°C. The loadings were quantified by measuring the amount of unloaded Fe(TDCPP)<sup>+</sup> in the combined reaction solvent and washings by UV–VIS spectroscopy.

## 2.2. UV–VIS spectra

The UV–VIS spectra were recorded on a Hewlett Packard 8452 Diode Array UV–VIS spectrophotometer. In the case of Fe(TDCPP)SG and Fe(TDCPP)IPG, spectra were recorded in a 2 mm path length quartz cell from Hellma, using a suspension of either the supported catalyst or a mixture of the supported catalyst and the support itself in  $\text{CCl}_4$ . The 'blank' was recorded previously and consisted of a support/ $\text{CCl}_4$  suspension. In the case of  $\text{Fe(TDCPP)}^+$  in homogeneous solutions, the spectra were recorded using either a 1.0 cm or 0.2 cm path length cell.

## 2.3. EPR spectra

The EPR spectra were recorded in a Varian E-109 century line spectrometer operating at the X-band. The  $g$  values were found by taking the frequency indicated in a HP 5340 A frequency meter and the field measured at the spectral features, which were recorded with increased gain and expanded field. Routine calibrations of the field setting and scan were made with DPPH and  $\text{Cr}^{3+}$  reference signals. The Helitran (Oxford Systems) low temperature accessory was employed to obtain the spectra in the specified temperature range.

### 2.3.1. EPR spectra of $\text{Fe(TDCPP)}^+$ supported on IPG or SG

The EPR spectra of Fe(TDCPP)SG and Fe(TDCPP)IPG were recorded after adding 0.0400–0.0700 mg of the supported catalyst to an EPR tube containing 200  $\mu\text{L}$  DCE.

### 2.3.2. Titration of Fe(TDCPP)IPG with NO

The EPR tube containing  $\sim 0.0650$  g of Fe(TDCPP)IPG was deaerated with  $\text{N}_2$  for 1 h. Afterwards,  $\text{N}_2$  was removed with syringe. Then, with the aid of a plastic syringe, 1 mL NO (generated from the reaction between  $\text{Cu}^0$  and  $\text{HNO}_3$  in a special disposal) was added to the FePIP and the EPR spectrum was recorded.

This procedure was repeated for the addition of another 1 mL NO.

## 2.4. Hydroxylation reactions

The reactions were carried out in a 2 mL vial with an open top screw cap containing a silicone teflon coated septum. In a standard reaction, to the vial containing iodobenzene ( $\sim 0.50$ – $2.50$  mg) and Fe(TDCPP)IPG (0.0125–0.1000 g) under argon atmosphere, 100–400  $\mu\text{L}$  of the desired solvent and 100–400  $\mu\text{L}$  of cyclohexane were added and the flask was adapted in a dark chamber. The mixture was stirred by magnetic stirring, at room temperature. The product was extracted with 200  $\mu\text{L}$  of the desired solvent, followed by 5 min magnetic stirring, until 2 mL of extract was obtained. For the catalyst recycling experiments, Fe(TDCPP)IPG was washed 5 times with 200  $\mu\text{L}$  dichloroethane. This procedure was done to ensure that the remaining iodobenzene was totally removed from the catalyst. The catalyst was then dried for 3 h at  $60^\circ\text{C}$ , before the next recycling.

Control of all reactions was carried out under the same conditions but in the absence of FeP and all the reactions were carried out in triplicate.

### 2.4.1. Product analysis

The product was analyzed by gas chromatography using  $n$ -octanol as the internal standard. The yields were based on iodobenzene. Gas chromatographic analysis were performed on either a CG 37-002 gas chromatograph or a CG 500 gas chromatograph coupled to a CG 300 integrator. Nitrogen was used as the carrier gas with an hydrogen flame ionization detector. The inox column (length, 1.8 m; internal diameter, 3 mm) was packed with 10% Carbowax 20M on Chromosorb WHP. The attained products were analyzed by comparison of their retention times with authentic samples.

### 3. Results and discussion

#### 3.1. Characterization of Fe(TDCPP)SG through UV–VIS and EPR spectroscopies

##### 3.1.1. UV–VIS spectra

The UV–VIS spectrum of Fe(TDCPP)Cl in 1,2-dichloroethane solution presents absorption bands at  $\lambda = 416$  (Soret), 508, 578 and 644 nm (Fig. 3A). The three peaks present in the region of 500–700 nm are typical of high-spin Fe<sup>III</sup> porphyrins [30,31]. In turn, the spectrum of Fe(TDCPP)SG containing  $1.1 \times 10^{-6}$  mol Fe(TDCPP)<sup>+</sup> per gram of support recorded of its suspension in CCl<sub>4</sub> presents absorption bands at  $\lambda = 414$  (Soret), 486, 580 and 605 nm (Fig. 3C). Kobayashi et al. [28] and Balch et al. [29] have attributed the band at  $\lambda = 580$  nm present in the spectra of Fe(TPP)OCH<sub>3</sub> and Fe(TMP)OH, respectively, to the axial coordination of the FeP to oxygen. Therefore we interpret that the band at  $\lambda = 580$  nm in the spectrum of Fe(TDCPP)SG is due to the axial coordination of Fe(TDCPP)<sup>+</sup> to the oxygen atoms of the support upon catalyst loading to silica gel.

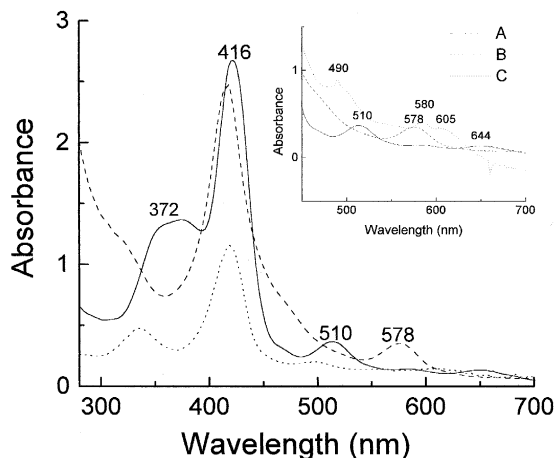


Fig. 3. UV–VIS spectra of (A)  $1.1 \times 10^{-7}$  mol Fe(TDCPP)Cl in 1,2-dichloroethane (in 1.0 cm path length cell); (B) (A) after the addition of  $7.5 \times 10^{-6}$  mol TBAOH,  $\text{OH}^-/\text{Fe}(\text{TDCPP})^+$  molar ratio = 6.8; (C) 0.0250 g of Fe(TDCPP)SG ‘diluted’ with 0.0750 g of SG corresponding to  $2.8 \times 10^{-8}$  mol Fe(TDCPP)<sup>+</sup> (dotted line) (in 0.2 cm path length cell).

To help characterize Fe(TDCPP)SG, solution models were investigated. We accompanied the titration of a 1,2-dichloroethane solution of Fe(TDCPP)Cl with an acetonitrile solution of tetrabutylammonium hydroxyde through UV–VIS spectroscopy (the procedures for such an experiment are described by us elsewhere [32]). Upon addition of excess  $\text{OH}^-$  ( $\text{OH}^-/\text{Fe}(\text{TDCPP})^+$  molar ratio = 6.8), the bands at  $\lambda = 508$  and 644 nm present in the spectrum of Fe(TDCPP)Cl (Fig. 3A) disappear and the band at 578 nm becomes more intense (Fig. 3B) [33]. The band at  $\lambda = 578$  nm is indicative of the coordination of Fe(TDCPP)<sup>+</sup> to  $\text{OH}^-$ , via oxygen. Using the method described by Fleischer et al. [34], we calculated the number of  $\text{OH}^-$  which is coordinated to Fe(TDCPP)<sup>+</sup> ( $n$ ) and the thermodynamic stability constant ( $\beta_n$ ) for the complex attained at the end of the titration. We found  $n = 2$  and  $\beta_n = 6.3 \times 10^7 \text{ mol}^{-2} \text{ L}^2$ , which leads to the conclusion that the very stable Fe(TDCPP)(OH)<sub>2</sub><sup>-</sup> complex was formed [33].

As the UV–VIS spectrum of Fe(TDCPP)SG is very similar to that of Fe(TDCPP)(OH)<sub>2</sub><sup>-</sup>, there is strong evidence that the band at  $\lambda = 580$  nm in the former is due to the Fe(TDCPP)<sup>+</sup>– $\text{OH}^-$  coordination. The absorption bands at  $\lambda = 486$  and 605 nm present in the spectrum of Fe(TDCPP)SG might be due to extraneous peaks from the support [25].

##### 3.1.2. EPR spectra

To continue the characterization of Fe(TDCPP)SG, EPR spectra of Fe(TDCPP)Cl in 1,2-dichloroethane solution, Fe(TDCPP)(OH)<sub>2</sub><sup>-</sup> and Fe(TDCPP)SG were recorded, aiming at assigning the iron ion oxidation and spin states in each case.

The EPR spectrum of Fe(TDCPP)Cl presents signals in  $g_{\perp} = 5.985$  and  $g_{\parallel} = 1.996$ , typical of high-spin Fe<sup>III</sup> species (Fig. 4A). The distorted  $g_{\perp} = 5.985$  signal is due to the coexistence of two complexes: Fe(TDCPP)Cl containing an axially coordinated solvent molecule and

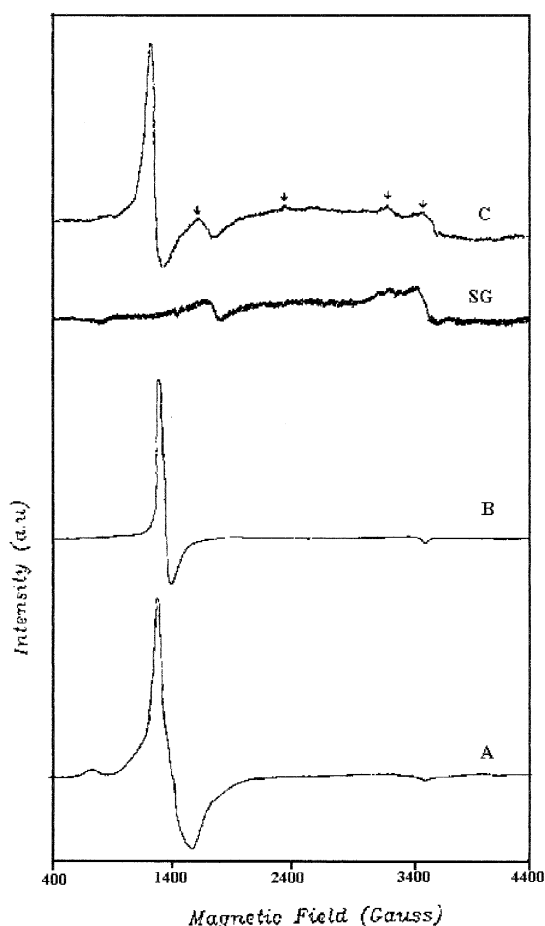


Fig. 4. EPR spectra of (A)  $\text{Fe}(\text{TDCPP})\text{Cl}$  (100 mL,  $8.6 \times 10^{-4}$  mol  $\text{L}^{-1}$ ) in DCE, gain =  $8.0 \times 10^2$ ; (B) (A) after the addition of  $2.1 \times 10^{-6}$  mol TBAOH, gain =  $2.5 \times 10^2$ ; (C) 0.0759 g of  $\text{Fe}(\text{TDCPP})\text{SG}$  containing  $1.1 \times 10^{-6}$  mol  $\text{Fe}(\text{TDCPP})^+/\text{g}$  SG, gain =  $1.6 \times 10^4$  ( $\downarrow$  extraneous peaks from the support); (SG) pure SG, gain =  $1.6 \times 10^4$ . EPR spectrometer conditions:  $T = 4.5\text{--}5.5$  K, microwave frequency = 9.240 GHz.

a bis-methanol  $\text{Fe}(\text{TDCPP})$  complex. The latter complex may have been formed during the  $\text{Fe}(\text{TDCPP})^+$  purification process (see Section 2.1.2) and its EPR  $g_{\perp} = 5.985$  narrow signal is superimposed by the distorted  $g_{\perp} = 5.985$  signal of  $\text{Fe}(\text{TDCPP})\text{Cl}$  containing a coordinated solvent molecule.

Upon addition of excess  $\text{OH}^-$  to  $\text{Fe}(\text{TDCPP})\text{Cl}$ , the signal in  $g_{\perp} = 5.985$  becomes more intense and highly symmetric and no low-spin  $\text{Fe}^{\text{III}}$  signals appear, indicating that the hexacoordinated high-spin

$\text{Fe}(\text{TDCPP})(\text{OH})_2^-$  complex was formed (Fig. 4B) [33]. In turn, the EPR spectrum of  $\text{Fe}(\text{TDCPP})\text{SG}$  (Fig. 4C) presents signal in  $g_{\perp} = 5.985$ , typical of high-spin  $\text{Fe}^{\text{III}}$  species. The high intensity and symmetry of the signal indicate that  $\text{Fe}(\text{TDCPP})^+$  may be axially bis-coordinated to oxygen atoms from the support. This suggestion is based on the fact that the EPR spectrum of  $\text{Fe}(\text{TDCPP})\text{SG}$  is similar to that of  $\text{Fe}(\text{TDCPP})(\text{OH})_2^-$ , except for the fact that the  $g_{\perp} = 5.985$  in the former is wider than in the latter, due to the fact that the supported catalyst constitutes a more rigid system. The extra lines in spectrum 4C are due to the support SG.

### 3.2. Characterization of $\text{Fe}(\text{TDCPP})\text{IPG}$ through UV–VIS and EPR spectroscopies. Influence of the iron porphyrin oxidation and spin states in the catalytic activity of $\text{Fe}(\text{TDCPP})\text{IPG}$

#### 3.2.1. UV–VIS spectra

To help characterize  $\text{Fe}(\text{TDCPP})\text{IPG}$ , solution models were investigated. We accompanied the titration of a 1,2-dichloroethane solution of  $\text{Fe}(\text{TDCPP})\text{Cl}$  (Fig. 5A) with a 1,2-dichloroethane solution of imidazole, through UV–VIS spectroscopy. Upon addition of excess imida-

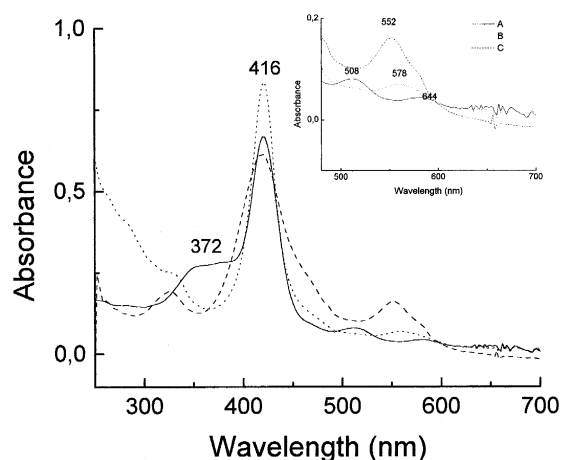


Fig. 5. UV–VIS spectra of (A)  $2.9 \times 10^{-8}$  mol  $\text{Fe}(\text{TDCPP})\text{Cl}$  in 1,2-dichloroethane; (B) A after the addition  $1.1 \times 10^{-7}$  mol imidazole,  $\text{Im}/\text{Fe}(\text{TDCPP})^+$  molar ratio = 3.8; (C) 0.0250 g of  $\text{Fe}(\text{TDCPP})\text{IPG}$  1 'diluted' with 0.0750 g of IPG corresponding to  $2.8 \times 10^{-8}$  mol  $\text{Fe}(\text{TDCPP})^+$  (0.2 cm path length cell).

zole (Im/Fe(TDCPP)<sup>+</sup> molar ratio = 3.8), the bands at  $\lambda = 508, 578$  and  $644$  nm present in the spectrum of high-spin Fe(TDCPP)Cl were replaced by a single absorption band at  $\lambda = 552$  nm and the Soret band shifted from  $416$  to  $418$  nm (Fig. 5B). It is well documented that the addition of nitrogen bases to solution of high-spin Fe<sup>III</sup> porphyrins leads to the formation of bis-ligated, low-spin Fe<sup>III</sup> porphyrins, which is accompanied by the replacement of the three absorption bands between  $500$ – $700$  nm by a single absorption band at  $\lambda = 550$  nm [31]. Therefore, the band at  $\lambda = 552$  nm present in the spectrum of Fe(TDCPP)<sup>+</sup> in the face of excess imidazole gives an indication that this FeP might bis-coordinate to this ligand. Using the method described by Fleischer et al. [34], we calculated the number of imidazole molecules that is coordinated to Fe(TDCPP)<sup>+</sup> ( $n$ ) and the thermodynamic stability constant ( $\beta_n$ ) for the complex obtained at the end of the titration. We found  $n = 2$  and  $\beta_n = 2.5 \times 10^8 \text{ mol}^{-2} \text{ L}^2$ , which confirm that the very stable Fe(TDCPP)(Im)<sub>2</sub><sup>+</sup> complex was formed. Despite the bulky chloro-substituents in its *ortho*-mesoaryl positions, Fe(TDCPP)<sup>+</sup> presents great tendency to bis-coordinate to imidazole [31]. This happens because the electronwithdrawing substituents in this FeP make the ferric ion very electrophilic, which leads to a great affinity of this ion for bases capable of donating electrons through resonance effects [31].

In turn, we recorded UV–VIS spectra of

various Fe(TDCPP)IPG (Table 1; Fe(TDCPP)IPG 1–5) containing different amounts of Fe(TDCPP)<sup>+</sup> and imidazole per gram of support, of their respective suspensions in CCl<sub>4</sub>. All the different Fe(TDCPP)IPG gave rise to UV–VIS spectra of similar pattern and in Fig. 5C we present the spectrum of Fe(TDCPP)IPG 1, which contains  $1.1 \times 10^{-6}$  mol Fe(TDCPP)<sup>+</sup> and  $2.2 \times 10^{-4}$  mol imidazole per gram support [24]. Fe(TDCPP)IPG presents absorption bands at  $\lambda = 420$  (Soret) and  $552$  nm (Fig. 5C). Since the spectrum of Fe(TDCPP)IPG is very similar to that obtained for Fe(TDCPP)(Im)<sub>2</sub><sup>+</sup>, we conclude that Fe(TDCPP)<sup>+</sup> binds to IPG through coordination to the imidazole present on the support. Moreover, the red shift of the Soret band from  $416$  nm in the initial Fe(TDCPP)Cl to  $420$  nm in Fe(TDCPP)IPG gives evidence that the reduction Fe<sup>III</sup>/Fe<sup>II</sup> may be occurring in the supported iron porphyrin [28].

However, UV–VIS spectra themselves are not conclusive as to whether the Fe(TDCPP)<sup>+</sup> is mono- or bis-coordinated to the support. For that reason we also utilized EPR spectroscopy to characterize the various Fe(TDCPP)IPG.

### 3.2.2. EPR spectra and catalytic activity

To continue the characterization of Fe(TDCPP)IPG, EPR spectra of Fe(TDCPP)Cl in 1,2-dichloroethane solution, Fe(TDCPP)(Im)<sub>2</sub><sup>+</sup> and Fe(TDCPP)IPG suspended in dichloromethane were recorded. As

Table 1  
EPR signals and catalytic activity in cyclohexane oxidation of Fe(TDCPP)SG and various Fe(TDCPP)IPG

Catalyst	Mol Fe(TDCPP) <sup>+</sup> / g support	Mol Im/g support	Im/Fe (TDCPP) <sup>+</sup>	Col (%) <sup>a</sup>	EPR signals
Fe(TDCPP)SG	$5.8 \times 10^{-7}$	—	—	17	$g_{\perp} = 5.985$
Fe(TDCPP)IPG 1	$1.1 \times 10^{-6}$	$2.2 \times 10^{-4}$	$2.0 \times 10^2$	28	$g_z = 2.983; g_y = 2.299$
Fe(TDCPP)IPG 2	$4.9 \times 10^{-6}$	$2.2 \times 10^{-4}$	$4.5 \times 10$	48	$g_z = 2.983; g_y = 2.299; g_{\perp} = 5.985$
Fe(TDCPP)IPG 3	$1.3 \times 10^{-6}$	$2.2 \times 10^{-5}$	$1.7 \times 10$	33	$g_z = 2.983; g_y = 2.299$
Fe(TDCPP)IPG 4	$3.3 \times 10^{-6}$	$2.2 \times 10^{-5}$	6.7	53	$g_z = 2.983; g_y = 2.299; g_{\perp} = 5.985$
Fe(TDCPP)IPG 5	$4.5 \times 10^{-6}$	$2.2 \times 10^{-5}$	4.9	67	$g_z = 2.983; g_y = 2.299; g_{\perp} = 5.985$

Conditions: argon atmosphere;  $T = 25^{\circ}\text{C}$ ; PhIO/Fe(TDCPP)<sup>+</sup> molar ratio = 17; magnetic stirring; reaction time = 1 h; solvent for reaction and product extraction: 1,2-dichloroethane.

<sup>a</sup> Based on PhIO.



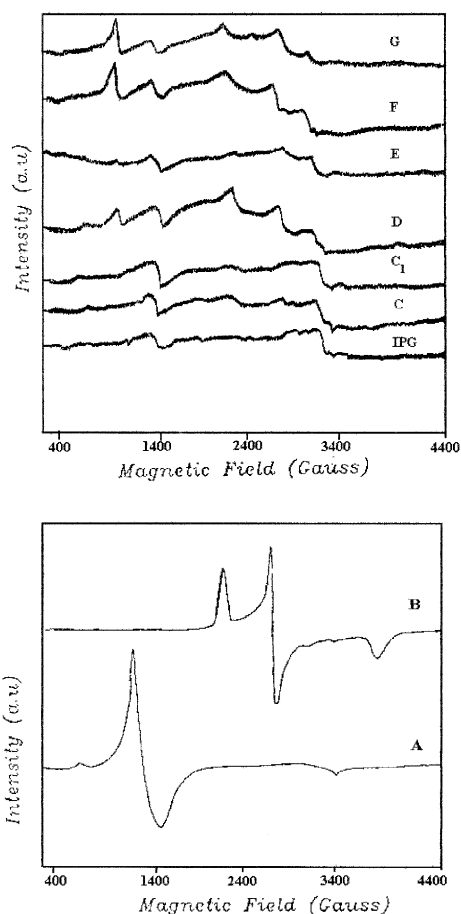


Fig. 6. EPR spectra of (A) Fe(TDCPP)Cl (100 mL,  $8.6 \times 10^{-4}$  mol L $^{-1}$ ) in DCE, gain =  $8.0 \times 10^2$ ; (B) (A) after the addition of  $1.85 \times 10^{-5}$  mol imidazole, gain =  $2.0 \times 10^3$ ; (IPG) pure IPG, gain =  $1.6 \times 10^4$ ; (C) 0.0715 g Fe(TDCPP)IPG 1, gain =  $1.6 \times 10^4$ ; (C<sub>1</sub>) Fe(TDCPP)IPG 1 after the addition of  $6.4 \times 10^{-5}$  mol imidazole, gain =  $1.6 \times 10^4$ ; (D) 0.0729 g Fe(TDCPP)IPG 2, gain =  $1.6 \times 10^4$ ; (E) 0.0766 g Fe(TDCPP)IPG 3, gain =  $1.0 \times 10^4$ ; (F) 0.0771 g Fe(TDCPP)IPG 4, gain =  $1.6 \times 10^4$ ; (G) 0.0669 g Fe(TDCPP)IPG 5, gain =  $6.3 \times 10^3$ . EPR spectrometer conditions:  $T = 4.5$ – $5.5$  K, microwave frequency 9.240 GHz.

already mentioned, Fe(TDCPP)Cl presents EPR signals in  $g_{\perp} = 5.985$  and  $g_{\parallel} = 1.996$ , typical of high-spin Fe<sup>III</sup> porphyrins (Fig. 6A). The distorted  $g_{\perp} = 5.985$  signal shows that Fe(TDCPP)<sup>+</sup> is present as a mixture of bis-methanol Fe(TDCPP) complex and Fe(TDCPP)Cl containing an axially coordinated solvent molecule.

Upon addition of excess imidazole, the high-spin Fe<sup>III</sup> signals disappear and low-spin Fe<sup>III</sup>

signals in  $g_z = 2.54$ ,  $g_y = 2.15$  and  $g_x = 1.90$  appear (Fig. 6B). This indicates the formation of the low-spin bis-imidazole complex Fe(TDCPP)(Im)<sub>2</sub><sup>+</sup>.

We then characterized various Fe(TDCPP)IPG containing different amounts of Fe(TDCPP)<sup>+</sup> and imidazole per gram support (Fig. 6C–G; Table 1, Fe(TDCPP)IPG 1–5), through EPR spectroscopy. The elucidation of the iron oxidation and spin states in such catalysts have helped us to better understand the different catalytic results attained using Fe(TDCPP)IPG 1 to 5 as catalyst in the oxidation of cyclohexane by PhIO. The results are presented in Table 1 and the EPR spectra in Fig. 6.

In a previous work [24], we had already reported the characterization of Fe(TDCPP)IPG 1, 2 and 4 (Fig. 6C, D and F, respectively) by EPR spectroscopy. Nevertheless, we have decided to present their respective spectra again in this report, in order to facilitate the discussion. Fe(TDCPP)IPG 1 (Fig. 6C) presents weak EPR signals in  $g_z = 2.983$  and  $g_y = 2.299$  ( $g_x$  not determined), due to the presence of a small amount of low-spin Fe<sup>III</sup> species. This differs from what has been observed for Fe(TPP)IPG containing the same amount of FeP and imidazole per gram of support, whose EPR spectrum presents high-spin Fe<sup>III</sup> EPR signals in  $g_{\perp} = 5.985$  and  $g_{\parallel} = 1.996$  [24]. Only in the face of excess imidazole do the high-spin signals in the spectrum of Fe(TPP)IPG disappear and they are replaced by the corresponding low-spin Fe<sup>III</sup> signals [24]. Therefore, the EPR spectrum of Fe(TDCPP)IPG 1 is very similar to that of Fe(TPP)IPG in the presence of excess imidazole and indicates that Fe(TDCPP)<sup>+</sup> bis-coordinates to the imidazole present on the support, forming stable bis-imidazolyl complexes. If excess imidazole is added to Fe(TDCPP)IPG 1, the EPR spectrum does not change (Fig. 6C<sub>1</sub>). Thus, there is indication that Fe<sup>II</sup> species are present in Fe(TDCPP)IPG 1, as they do not present EPR signals [35–37]. We considered that in this case, a reductive addition in the bis-imidazole

complex may be occurring in the basic medium, since the central ferric ion in  $\text{Fe}(\text{TDCPP})^+$  is very electrophilic due to the presence of the chloro-substituents and so, is more susceptible to nucleophilic attack [38,39].

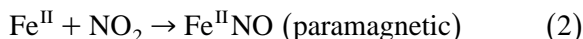
In order to confirm the presence of  $\text{Fe}^{\text{II}}$  species in  $\text{Fe}(\text{TDCPP})\text{IPG } \mathbf{1}$ , we have accompanied a titration of this catalyst with NO, by EPR spectroscopy. It is well-known that NO functions as a paramagnetic probe for iron ions because [35,36]:

(a) NO coordinates to high or low-spin  $\text{Fe}^{\text{III}}$ , which is paramagnetic, to give  $\text{Fe}^{\text{II}}\text{NO}^+$ , which is diamagnetic and thus, EPR silent,

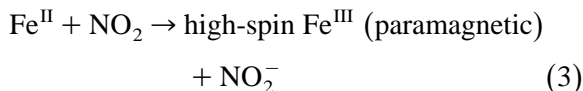
$\text{Fe}^{\text{III}}$  (paramagnetic) + NO



(b) NO coordinates to  $\text{Fe}^{\text{II}}$ , which does not present EPR signals [37], to give  $\text{Fe}^{\text{II}}\text{NO}$ , which is paramagnetic, spin 1/2 and presents EPR signals in  $g \sim 2$ ,



(c) NO may react with  $\text{O}_2$  giving  $\text{NO}_2$ , which in turn reacts with  $\text{Fe}^{\text{II}}$  to give high-spin  $\text{Fe}^{\text{III}}$  and  $\text{NO}_2^-$ ,



By adding NO to  $\text{Fe}(\text{TDCPP})\text{IPG } \mathbf{1}$  (Fig. 7A), weak signals in  $g \sim 2$  typical of  $\text{Fe}^{\text{II}}\text{NO}$  [35,36] species were observed (Fig. 7B–D). These species are provenient from the reaction between  $\text{Fe}^{\text{II}}$  and NO (Eq. (2)). However, this reaction did not occur to a great extent because very little NO coordinated to  $\text{Fe}^{\text{II}}$  due to the fact that excess imidazole in  $\text{Fe}(\text{TDCPP})\text{IPG } \mathbf{1}$  partially blocked such coordination. The NO system was not efficient enough to avoid the contact between NO and  $\text{O}_2$ , which led to the formation of  $\text{NO}_2$ , a brownish gas. Upon addition of 1 mL of NO contaminated with  $\text{NO}_2$  to  $\text{Fe}(\text{TDCPP})\text{IPG } \mathbf{1}$  (Fig. 7A), the appearance of a low intensity signal in  $g_{\perp} = 5.985$  was also observed (Fig. 7B). This once more indicates

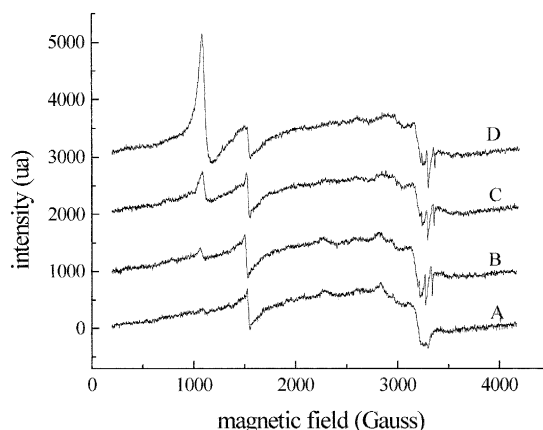
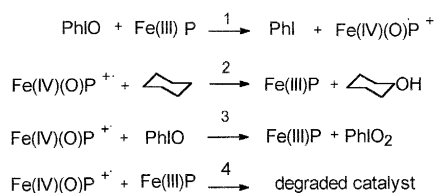


Fig. 7. Titration of  $\text{Fe}(\text{TDCPP})\text{IPG } \mathbf{1}$  (containing  $1.2 \times 10^{-6}$  mol  $\text{Fe}(\text{TDCPP})^+$  and  $2.2 \times 10^{-4}$  mol Im/g IPG) with NO accompanied by EPR spectroscopy. (A) initial 0.0640 g  $\text{Fe}(\text{TDCPP})\text{IPG } \mathbf{1}$ ; (B) (A) after addition of 1 mL NO containing  $\text{NO}_2$ ; (C) (A) after addition of 2 mL NO containing  $\text{NO}_2$ ; (D) (C) after 1 h. EPR spectrometer conditions:  $T = 4.5\text{--}5.5$  K, microwave frequency 9.240 GHz, gain =  $6.3 \times 10^3$ .

that there are  $\text{Fe}^{\text{II}}$  species in  $\text{Fe}(\text{TDCPP})\text{IPG } \mathbf{1}$ , which react with  $\text{NO}_2$  to furnish high-spin  $\text{Fe}^{\text{III}}$  species (Eq. (3)). Upon addition of another 1 mL of NO contaminated with  $\text{NO}_2$  to  $\text{Fe}(\text{TDCPP})\text{IPG } \mathbf{1}$ , the high-spin  $\text{Fe}^{\text{III}}$  signal increased, indicating that more high-spin  $\text{Fe}^{\text{III}}$  species were formed from  $\text{Fe}^{\text{II}}$  (Fig. 7C). After leaving the mixture to react for more 1 h, the high-spin  $\text{Fe}^{\text{III}}$  signal in  $g_{\perp} = 5.985$  increased even more since, during this time, the contact between NO and  $\text{O}_2$  led to the formation of  $\text{NO}_2$ , which in turn converted  $\text{Fe}^{\text{II}}$  present in  $\text{Fe}(\text{TDCPP})\text{IPG } \mathbf{1}$  to high-spin  $\text{Fe}^{\text{III}}$  species.

Further on, we recorded an EPR spectrum of  $\text{Fe}(\text{TDCPP})\text{IPG } \mathbf{3}$ , which contains the same amount of  $\text{Fe}(\text{TDCPP})^+$  as  $\text{Fe}(\text{TDCPP})\text{IPG } \mathbf{1}$  (Fig. 6C), but less imidazole, which means a lower Im/ $\text{Fe}(\text{TDCPP})^+$  molar ratio (Table 1 and Fig. 6E). The spectrum of  $\text{Fe}(\text{TDCPP})\text{IPG } \mathbf{3}$  is very similar to that of  $\text{Fe}(\text{TDCPP})\text{IPG } \mathbf{1}$ . Despite having a lower Im/ $\text{Fe}(\text{TDCPP})^+$  molar ratio, the amount of  $\text{Fe}(\text{TDCPP})^+$  in  $\text{Fe}(\text{TDCPP})\text{IPG } \mathbf{3}$  is not sufficient to avoid its bis-coordination to imidazole on the support and, consequently, the conversion high-spin  $\text{Fe}^{\text{III}}$ /low-spin  $\text{Fe}^{\text{III}}$  and the reduction  $\text{Fe}^{\text{III}}$ / $\text{Fe}^{\text{II}}$ .



where: Fe(III)P = iron (III)porphyrin, Fe(IV)(O)P<sup>·+</sup> = catalytic species I,  
PhIO<sub>2</sub> = iodoxybenzene, PhIO = iodosylbenzene, PhI = iodobenzene

Fig. 8. Mechanism for the hydroxylation of cyclohexane by PhIO and iron(III)porphyrin and possible competitive reactions [40].

With the characterization of Fe(TDCPP)IPG **1** and **3**, it is now easier to understand why their catalytic activities are relatively low (Table 1; Col yields (%) = 28 and 33, respectively). The active catalytic species Fe<sup>IV</sup>(O)P<sup>·+</sup>, responsible for the transference of the oxygen atom from PhIO to cyclohexane is usually generated from the reaction between Fe<sup>III</sup> porphyrin and PhIO (Fig. 8) [40]. However, in the above mentioned Fe(TDCPP)IPG, all the Fe<sup>III</sup>P species are low-spin and bis-ligated to imidazole, which partially hinders the reaction between Fe(TDCPP)<sup>+</sup> and PhIO. So with these catalysts, the active species Fe<sup>IV</sup>(O)P<sup>·+</sup> must be slowly formed, and in low amounts, from the low-spin Fe<sup>III</sup> species, while Fe<sup>II</sup>P does not react with PhIO. This leads to low yields of cyclohexanol.

By increasing the amount of Fe(TDCPP)<sup>+</sup> on the support, as in the case of Fe(TDCPP)IPG **2** (Fig. 6D), a high-spin EPR Fe<sup>III</sup> signal in  $g_{\perp} = 5.985$  accompanied by low-spin Fe<sup>III</sup> signals in  $g_z = 2.878$  and  $g_y = 2.299$  ( $g_x$  not determined) were observed [24]. Cyclohexanol yields of 48% were attained with this catalyst (Table 1). By decreasing the amount of imidazole on the support, as was done for Fe(TDCPP)IPG **4** [24] and **5** (Fig. 6F and G, respectively), an even more intense high-spin Fe<sup>III</sup> signal is attained, accompanied by less intense low-spin Fe<sup>III</sup> signals. When one observes the yields of cyclohexanol using Fe(TDCPP)IPG **3**, **4** and **5**, it can be noticed that the catalytic activity increases in the order Fe(TDCPP)IPG **3** < **4** < **5** (Table 1, Col yields (%) = 48, 53 and 67, respectively).

This leads to the conclusion that the higher the amount of high-spin Fe<sup>III</sup> species on the support, the better the catalytic activity. Therefore, the rate of Fe<sup>IV</sup>(O)P<sup>·+</sup> formation depends on the amount of high-spin Fe<sup>III</sup> species present on the support.

After this characterization study, one can conclude that in Fe(TDCPP)IPG, the central ion is so electrophilic that, when there is a high Im/Fe(TDCPP)<sup>+</sup> molar ratio, some of the FeP tends to bis-coordinate to the imidazole present on the support and/or be reduced to Fe<sup>II</sup>. This electrophilicity is due to the presence of the chlorosubstituents in the *ortho*-mesoaryl positions of the porphyrin ring. Moreover, when there is a low Im/Fe(TDCPP)<sup>+</sup> molar ratio, some of the FeP still tends to bis-coordinate to the imidazole present on the support, as can be seen by the  $g_z = 2.983$  and  $g_y = 2.299$  ( $g_x$  not determined) EPR signals present in the spectra of Fe(TDCPP)IPG **2**, **4** and **5** (Fig. 6D, F and G, respectively). Nevertheless, the tendency to FeP bis-coordination seems not to be so much dependent on Im/Fe(TDCPP)<sup>+</sup> molar ratio as it is on the amount of Fe(TDCPP)<sup>+</sup> per gram support. For example, despite the fact that Fe(TDCPP)IPG **3** (Fig. 6E) has a lower Im/Fe(TDCPP)<sup>+</sup> molar ratio than Fe(TDCPP)IPG **2** (Fig. 6D) ( $1.7 \times 10$  and  $4.5 \times 10$ , respectively), it does not contain high-spin Fe<sup>III</sup> species. This may happen because the lower amount of Fe(TDCPP)<sup>+</sup> in Fe(TDCPP)IPG **3** may not be sufficient to avoid bis-coordination of FeP to the support, in the face of excess imidazole.

An EPR study of the titration of Fe(TDCPP)IPG **5** with NO in order to compare its behavior in the face of this ligand with that of Fe(TDCPP)IPG **1** is in current progress in our laboratory.

### 3.3. Comparison between the catalytic activities of Fe(TDCPP)SG and Fe(TDCPP)IPG **1**

In a previous work [24], we had already presented catalytic results using both

Fe(TDCPP)SG and Fe(TDCPP)IPG **1**. In this report, we intend to draw a discussion comparing the activity of both catalysts in the oxidation of cyclohexane by PhIO.

The catalytic activity of Fe(TDCPP)SG is lower than the catalytic activity of Fe(TDCPP)IPG **1** (Table 1). We had suggested in Section 3.1 that Fe(TDCPP)<sup>+</sup> might be bis-coordinated to the support, due to the intense and symmetric high-spin signal in  $g_{\perp} = 5.985$  present in the EPR spectrum of Fe(TDCPP)SG (Fig. 4C). The low cyclohexanol yields attained in the presence of this catalyst give us a further indication that this bis-coordination might in fact occur. If the FeP 6th coordination position is occupied by its ligation to silica gel, the approach between PhIO and Fe(TDCPP)<sup>+</sup> is difficult, the active species Fe<sup>IV</sup>(O)P<sup>·+</sup> is not formed and consequently cyclohexanol is not produced. Moreover, Gunter and Turner [41] report that when FeP is bis-coordinated to oxygen atoms, the strong  $\pi$  donation from the ligand causes the catalytic efficiency to be lower because the electrophilicity of the Fe<sup>IV</sup>(O)P<sup>·+</sup> active species is decreased. Consequently, the reactivity of the active species towards cyclohexane also decreases. This  $\pi$  donation is possible in the case of ligands containing oxygen because the p orbitals of this atom have suitable energy to interact with the orbitals of high-spin Fe<sup>III</sup> porphyrins.

On the other hand, presence of imidazole on the support leads to better catalytic activity. This happens because imidazole donates elec-

trons to the iron ion in Fe(TDCPP)<sup>+</sup> through  $\sigma$  charge donation, causing the Fe–O bond in the active intermediate Fe<sup>IV</sup>(O)P<sup>·+</sup> to weaken. This intermediate, in turn, transfers the oxygen atom to cyclohexane more easily. However, the catalytic activity of Fe(TDCPP)IPG is only satisfactory if the amount of Fe(TDCPP)<sup>+</sup> on the support is enough to prevent its bis-coordination to imidazole in excess and/or Fe<sup>III</sup> reduction. In that way, most of the Fe(TDCPP)<sup>+</sup> present on the support will be mono-coordinated to imidazole and high-spin Fe<sup>III</sup> species, which gives rise to Fe<sup>IV</sup>(O)P<sup>·+</sup> in the presence of PhIO.

### 3.4. Optimization of reaction conditions for Fe(TDCPP)IPG–PhIO systems in the oxidation of cyclohexane

We have chosen cyclohexane as substrate because the great inertness of its C–H bonds provides information about the nature, reactivity and stability of the active species Fe<sup>IV</sup>(O)P<sup>·+</sup>. If a catalyst is capable of oxidizing this substrate giving rise to high yields of cyclohexanol, it is because it is very efficient. We have carried out the optimization study taking into account the following factors: PhIO and Fe(TDCPP)<sup>+</sup> concentration, PhIO/Fe(TDCPP)<sup>+</sup> molar ratio and reaction time.

#### 3.4.1. Fe(TDCPP)<sup>+</sup> and PhIO concentration and PhIO / Fe(TDCPP)<sup>+</sup> molar ratio

Having attained better yields with Fe(TDCPP)IPG **5** (Table 1, Col (%) = 67), we

Table 2  
Influence of Fe(TDCPP)<sup>+</sup> and PhIO concentration and PhIO/Fe(TDCPP)<sup>+</sup> molar ratio in the catalytic activity of Fe(TDCPP)IPG **5**

Reaction	[Fe(TDCPP) <sup>+</sup> ] (mol L <sup>-1</sup> )	PhIO (mol L <sup>-1</sup> )	PhIO/Fe(TDCPP) <sup>+</sup> molar ratio	Col (%) <sup>a</sup>	Turnover
a	$1.2 \times 10^{-3}$	$2.1 \times 10^{-2}$	17	67	11
b	$3.0 \times 10^{-4}$	$5.0 \times 10^{-3}$	17	83	14
c	$3.0 \times 10^{-4}$	$1.8 \times 10^{-2}$	60	67	40
d	$3.0 \times 10^{-4}$	$3.0 \times 10^{-2}$	100	59	59
e	$7.6 \times 10^{-5}$	$7.6 \times 10^{-3}$	100	69	69

Conditions: argon atmosphere,  $T = 25^{\circ}\text{C}$ ,  $4.5 \times 10^{-6}$  mol Fe(TDCPP)<sup>+</sup> per gram support,  $2.2 \times 10^{-5}$  mol imidazole per gram support, magnetic stirring, reaction time = 1 h, solvent for reaction and product extraction: 1,2-dichloroethane.

<sup>a</sup> Based on PhIO.

continued our optimization study using this catalyst.

Lower concentrations of PhIO and  $\text{Fe}(\text{TDCPP})^+$  in these systems lead to better results because in this way, PhIO is better solubilized, making its reaction with  $\text{Fe}(\text{TDCPP})\text{IPG}$  easier and faster (Table 2, reactions a and b, Col (%) = 67 and 83, respectively).

A decrease in the yield of cyclohexanol can be observed when the  $\text{PhIO}/\text{Fe}(\text{TDCPP})^+$  molar ratio is increased (Table 2, reactions b, c and d, Col (%) = 83, 67 and 59, respectively). What seems to be happening is the competitive reaction between PhIO and cyclohexane for the active species  $\text{Fe}^{\text{IV}}(\text{O})\text{P}^+$  (Fig. 8) [40], leading to the formation of  $\text{PhIO}_2$ . In fact, an insoluble white solid was detected at the end of reaction d, where a high  $\text{PhIO}/\text{Fe}(\text{TDCPP})^+$  molar ratio was employed. Furthermore, when higher ratios are used, satisfactory PhIO solubilization may not be occurring. Despite the decrease in the cyclohexanol yields, higher catalyst turnover numbers have been attained for  $\text{Fe}(\text{TDCPP})\text{IPG}$  **5** through the use of high  $\text{PhIO}/\text{Fe}(\text{TDCPP})^+$  molar ratios.

Based on the previous observation that lower  $\text{Fe}(\text{TDCPP})^+$  and PhIO concentrations lead to higher cyclohexanol yields (Table 2, reactions a and b), we have tried to improve the yield of 59% (Table 2, reaction d) for  $\text{PhIO}/\text{Fe}(\text{TDCPP})^+$  molar ratio = 100, by diluting the reaction mixture (Table 2, reactions d and e, Col (%) = 59 and 69, respectively). Once more an increase in the yield of cyclohexanol was observed. Reaction e conditions were used for the following step.

### 3.4.2. Reaction time

The next step was to optimize the reaction time for the  $\text{Fe}(\text{TDCPP})\text{IPG}$  **5**-PhIO system. As can be seen in Fig. 9A, the catalytic activity of  $\text{Fe}(\text{TDCPP})\text{IPG}$  **5** reaches its maximum at 60 min of reaction and remains constant after this time. Therefore, after 1 h, the oxidation reaction has reached its completion.

Comparing the kinetic study for the catalysts

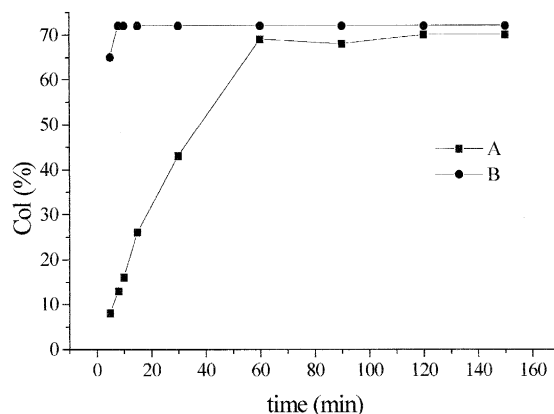


Fig. 9. Cyclohexanol yield  $\times$  reaction time in the oxidation of cyclohexane catalyzed by (A)  $\text{Fe}(\text{TDCPP})\text{IPG}$  **5**,  $[\text{Fe}(\text{TDCPP})^+] = 7.6 \times 10^{-5} \text{ mol L}^{-1}$  and  $\text{PhIO}/\text{Fe}(\text{TDCPP})^+$  molar ratio = 100, (B)  $\text{Fe}(\text{TDCPP})\text{Cl}$  in 1,2-dichloroethane,  $[\text{Fe}(\text{TDCPP})^+] = 3.0 \times 10^{-4} \text{ mol L}^{-1}$  and  $\text{PhIO}/\text{Fe}(\text{TDCPP})^+$  molar ratio = 17 [42].

$\text{Fe}(\text{TDCPP})\text{IPG}$  **5** and  $\text{Fe}(\text{TDCPP})\text{Cl}$  [42] (Fig. 9), it can be seen that the former is ten times slower than the latter. Lindsay [14] attributes this fact to the difference in polarity regarding the catalysts active sites. In  $\text{Fe}(\text{TDCPP})\text{IPG}$  **5**, the active site must be considerably more polar than that of  $\text{Fe}(\text{TDCPP})\text{Cl}$  in 1,2-dichloroethane. This may disfavor both the approach of the substrate cyclohexane, which is apolar, and the diffusion of the product cyclohexanol from the heterogenized catalyst to bulk solution. The latter factor explains the need for product extraction after the end of the reaction.

### 3.5. Study of the catalytic activity of $\text{Fe}(\text{TDCPP})\text{IPG}$ **5** in recycling experiments

In a previous work [24], we had studied the catalytic activity of  $\text{Fe}(\text{TDCPP})\text{IPG}$  **1** in recycling experiments. We had attained a total catalyst turnover number of 30. Knowing that  $\text{Fe}(\text{TDCPP})\text{IPG}$  **5**, in one single reaction leads to a turnover number of 69 when  $\text{PhIO}/\text{Fe}(\text{TDCPP})^+$  molar ratio = 100 is used (see Table 2, reaction d), we decided to carry out a study of this catalyst in repeat oxidation reactions. This study is shown in Table 3.

As already mentioned, unused Fe(TDCPP)IPG **5** leads to a cyclohexanol yield of 69% (Table 3, unused catalyst). When it is reused in a new oxidation reaction (Table 3, 1st recycle), it gives rise to a cyclohexanol yield of 66%. In other words, the catalyst maintained its activity upon a first reuse. Carrying on its further reuse, a total turnover number of 201 was obtained. However, in the conditions utilized, the yield of cyclohexanol decreased after the 1st recycle (Table 3, Col (%) = 35 and 31 for the 2nd recycle and 3rd recycle, respectively). Although Fe(TDCPP)<sup>+</sup> leaching from the support was not observed, the solid catalyst recovered after the first recycle was of a lighter orange color than the initial catalyst and changed from orange to green after the second and third recycles. Maybe a PhIO/Fe(TDCPP)<sup>+</sup> molar ratio as high as 100 has been a very drastic condition, leading to changes in Fe(TDCPP)IPG **5** which have caused its catalytic activity to decrease. Lindsay [14] attributes this decrease in the catalytic activity of supported Fe(TDCPP)<sup>+</sup> in the epoxidation of cyclooctene after successive recycles to a possible oxidative self-destruction of the FeP.

We therefore decided to carry out recycling oxidation reactions with Fe(TDCPP)IPG **5** using a lower PhIO/Fe(TDCPP)<sup>+</sup> molar ratio (17).

As can be seen in Table 3, with the unused catalyst, a yield of 83% was obtained and its 1st recycle led to a yield of 77%, which remained the same until the 5th recycle. However, in the 6th reuse of the catalyst, no cyclohexanol was attained, indicating that Fe(TDCPP)IPG **5** lost its activity and a total turnover number of 76 was achieved.

Although a PhIO/Fe(TDCPP)<sup>+</sup> molar ratio = 100 consisted in a drastic condition, it is better to utilize this higher ratio than a lower one because in the former condition, a higher total turnover number was attained. That is, Fe(TDCPP)IPG **5** is more efficiently utilized.

#### 4. Conclusions

The study of the interaction between Fe(TDCPP)<sup>+</sup> and the axial ligands OH<sup>-</sup> and imidazole through EPR and UV–VIS spectroscopies was of great help in the characterization of both Fe(TDCPP)SG and Fe(TDCPP)IPG, which allowed an understanding of their different catalytic activities.

Studies of Fe(TDCPP)IPG **1** through EPR using NO as a paramagnetic probe confirmed that in this catalyst, there are Fe<sup>II</sup>P species, as we had already reported in a previous work

Table 3  
Study of the catalytic activity of Fe(TDCPP)IPG **5** in recycling experiments

	PhIO/Fe(TDCPP) <sup>+</sup> molar ratio, [Fe(TDCPP)Cl] (mol L <sup>-1</sup> )			
	100, 7.6 × 10 <sup>-5</sup>		17, 3.0 × 10 <sup>-4</sup>	
	Col (%) <sup>a</sup>	turnover	Col (%) <sup>a</sup>	turnover
Fe(TDCPP)IPG <b>5</b>	69	69	83	14
1st	66	66	77	13
2nd	35	35	76	13
3rd	31	31	77	13
4th	<sup>b</sup>	—	65	11
5th	<sup>b</sup>	—	73	12
6th	<sup>b</sup>	—	0	0
	total turnover = 201		total turnover = 76	

Conditions: argon atmosphere,  $T = 25^\circ\text{C}$ , magnetic stirring,  $4.5 \times 10^{-6}$  mol Fe(TDCPP)<sup>+</sup> per gram support,  $2.2 \times 10^{-5}$  mol imidazole per gram support, reaction time = 1 h, solvent for reaction and product extraction and catalyst washing: 1,2-dichloroethane.

<sup>a</sup> Based on PhIO.

<sup>b</sup> Not carried out.

[24]. The characterization of the different Fe(TDCPP)IPG through EPR was of utmost importance in directing the study of optimization of the catalytic activity of this supported catalyst.

The optimization study of the reaction conditions for Fe(TDCPP)IPG led us to obtain a yield of cyclohexanol of 69% and a turnover number of 69 (Table 3, Fe(TDCPP)IPG 5, PhIO/Fe(TDCPP)<sup>+</sup> molar ratio = 100, [Fe(TDCPP)<sup>+</sup>] =  $7.5 \times 10^{-5}$  mol L<sup>-1</sup>). This result was far better than the first one reported by us (Col (%) = 25, turnover number = 4, Fe(TDCPP)IPG 1, PhIO/Fe(TDCPP)<sup>+</sup> molar ratio = 17, [Fe(TDCPP)<sup>+</sup>] =  $3.0 \times 10^{-4}$  mol L<sup>-1</sup>) [24] and the high selectivity of the catalyst giving cyclohexanol as the sole product was maintained.

The goal of this study can be noted by comparing the optimized result of the heterogenized catalyst with that for Fe(TDCPP)Cl in homogeneous solution [42] (Col (%) = 96%, turnover number = 96, PhIO/Fe(TDCPP)<sup>+</sup> molar ratio = 100, [Fe(TDCPP)<sup>+</sup>] =  $3.0 \times 10^{-4}$  mol L<sup>-1</sup>, ultrasound stirring at 0°C). Although the former is still lower than the latter, carrying out repeat oxidation reactions using the heterogenized catalyst leads to a total turnover number of 201 and a total cyclohexanol yield of 201%, which cannot be obtained with Fe(TDCPP)Cl in homogeneous solution due to the difficulty in recovering and reusing it. Moreover, the total turnover number of 201 was obtained with Fe(TDCPP)IPG 5 by using a lower catalyst concentration than that utilized for Fe(TDCPP)Cl in homogeneous solution ([Fe(TDCPP)<sup>+</sup>] =  $7.5 \times 10^{-5}$  and  $3.0 \times 10^{-4}$  mol L<sup>-1</sup>, respectively) and without need for low temperatures or ultrasound stirring [42].

## Acknowledgements

This work was supported by CAPES, CNPq and FAPESP. We are grateful to Eduardo J. Nassar for technical assistance, Osvaldo Anto-

nio Serra for helpful discussions and Y. Gushikem and M.S. Iamamoto for the initial studies and IPG preparations.

## References

- [1] B. Meunier, Bull. Soc. Chim. Fr. (1986) 578.
- [2] B. Meunier, Chem. Rev. 92 (1992) 1411.
- [3] D. Mansuy, P. Battioni and J.P. Battioni, Eur. J. Biochem. 184 (1989) 267.
- [4] D. Mansuy, Pure Appl. Chem. 59 (1987) 759.
- [5] J.R. Lindsay-Smith, in: R.A. Sheldon (Ed.), Metalloporphyrins in Catalytic Oxidations (Marcel Dekker Inc., New York, 1994) ch. 11.
- [6] D. Mansuy, Coord. Chem. Rev. 125 (1993) 129.
- [7] B.A. Arndtsen, R.G. Bergman, T.A. Mobley and T.H. Peterson, Acc. Chem. Res. 28 (1995) 154.
- [8] J.T. Groves, T.E. Nemo and R.S. Myers, J. Am. Chem. Soc. 101 (1979) 1032.
- [9] P.S. Traylor, D. Dolphin and T.G. Traylor, J. Chem. Soc. Chem. Commun. (1984) 279.
- [10] C.K. Chang and F. Ebina, J. Chem. Soc. Chem. Commun. (1981) 778.
- [11] T.G. Traylor and S. Tsuchiya, Inorg. Chem. 26 (1987) 1338.
- [12] A.W. Van der Made, J.W.H. Smeets, R.J.M. Nolte and W. Drenth, J. Chem. Soc. Chem. Commun. (1983) 1204.
- [13] P.R. Cooke and J.R.L. Smith, Tetrahedron Lett. 33 (1992) 2737.
- [14] C. Gilmartin and J.R.L. Smith, J. Chem. Soc. Perkin Trans. 2 (1995) 243.
- [15] P. Battioni, J.F. Bartoli, D. Mansuy, Y.S. Byun and T.G. Traylor, J. Chem. Soc. Chem. Commun. (1992) 1051.
- [16] E. Polo, R. Amadelli, V. Carassiti and A. Maldotti, Inorg. Chim. Acta Lett. 192 (1992) 1.
- [17] D.R. Leanord and J.R.L. Smith, J. Chem. Soc. Perkin Trans. 2 (1990) 1917.
- [18] L. Barloy, J.P. Lalier, P. Battioni and D. Mansuy, New J. Chem. 16 (1992) 71.
- [19] L. Barloy, P. Battioni and D. Mansuy, J. Chem. Soc. Chem. Commun. (1990) 1365.
- [20] T. Tatsumi, M. Nakamura and H. Tominaga, Catal. Today 6 (1989) 163.
- [21] O. Leal, D.L. Anderson, R.G. Bowman, F. Basolo and J. Burwell, Jr., J. Am. Chem. Soc. 97 (1975) 5125.
- [22] T. Tatsumi, M. Nakamura and H. Tominaga, Chem. Lett. (1989) 419.
- [23] P.R. Cooke and J.R.L. Smith, J. Chem. Soc. Perkin Trans. 1 (1994) 1913.
- [24] Y. Iamamoto, K.J. Ciuffi, H.C. Sacco, C.M.C. Prado, M. Moraes and O.R. Nascimento, J. Mol. Cat. 88 (1994) 167.
- [25] P.R. Cooke, C. Gilmartin, G.W. Gray and J.R.L. Smith, J. Chem. Soc. Perkin Trans. 2 (1995) 1573.
- [26] J.G. Sharefkin and H. Saltzmann, Org. Synth. 43 (1963) 62.
- [27] A.D. Adler, F.R. Longo, F. Kampas and J. Kim, J. Inorg. Nucl. Chem. 32 (1970) 2443.
- [28] H. Kobayashi, Y. Yanagawa, H. Osada, S. Minami and M. Shimizu, Bull. Chem. Soc. Jpn. 46 (1973) 1471.

- [29] R.J. Cheng, L. Latos-Grazynski and A.L. Balch, *Inorg. Chem.* 21 (1982) 2412.
- [30] D. Dolphin, *The Porphyrins*, Vol. III (Academic Press, New York, 1978).
- [31] K. Hatano, M.K. Safo, F. Ann Walker and W.R. Scheidt, *Inorg. Chem.* 30 (1991) 1643.
- [32] L.S. Iwamoto, Master Dissertation, University of São Paulo, Brazil (1993); O.A. Serra, Y. Iamamoto and L.S. Iwamoto, *International Conference on Coordination Chemistry, Lausanne, Switzerland*, V. 29 (1992) p. 74.
- [33] C.M.C. Prado, H.C. Sacco, K.J. Ciuffi and Y. Iamamoto *Química Nova*, Supl. 17, QI 13 (1994); C.M.C. Prado, L.S. Iwamoto, O.A. Serra and Y. Iamamoto, *Química Nova*, Supl. 18, QI-28 (1995).
- [34] E.B. Fleischer and D.A. Fine, *Inorg. Chim. Acta* 29 (1978) 267.
- [35] L. Martin Neto, O.R. Nascimento, M. Tabak and I. Caracelli, *Biochim. and Biophys. Acta* 956 (1988) 189.
- [36] L. Martin Neto, O.R. Nascimento and M. Tabak, *J. Inorg. Biochem.* 40 (1990) 309.
- [37] J. Subramanian, in: K.M. Smith (Ed.), *Porphyrins and metalloporphyrins* (Elsevier Scientific Publishing Company, Amsterdam, 1975) p. 571.
- [38] D.T. Sawyer and J.L. Roberts, Jr., *Acc. Chem. Res.* 21 (1988) 469.
- [39] S. Modi, V.P. Shedbakar and D.V. Behere, *Inorg. Chim. Acta* 173 (1990) 9.
- [40] M.J. Nappa and C.A. Tolman, *Inorg. Chem.* 24 (1985) 4711.
- [41] M.J. Gunter and P. Turner, *Coord. Chem. Rev.* 108 (1991) 115.
- [42] Y. Iamamoto, M.D. Assis, K.J. Ciuffi, H.C. Sacco, L.S. Iwamoto, A.J.B. Melo, O.R. Nascimento and C.M.C. Prado, *J. Mol. Catal. A* 109 (1996) 189.